



Supplement of

Isoprene emission potentials from European oak forests derived from canopy flux measurements: an assessment of uncertainties and inter-algorithm variability

Ben Langford et al.

Correspondence to: Ben Langford (benngf@ceh.ac.uk)

The copyright of individual parts of the supplement might differ from the CC BY 3.0 License.

S1.1 Alice Holt – Measurement setup

Above canopy-isoprene flux measurements at the Alice Holt forest site were made by combining fast measurements of isoprene made using a proton transfer reaction mass spectrometer (PTR-MS, Ionicon Analytik GmbH, Innsbruck, Austria), with measurements of the vertical wind velocity, made using a Gill Solent (R1012A) ultrasonic anemometer mounted atop a 25 m tall lattice tower at a height of 28.5 m. The PTR-MS was housed in a small container at the base of the tower and subsampled air from a 30 m PTFE tube (1/2" OD, 3/8" ID) which drew air from directly below the anemometer at a rate of 60 L min⁻¹ to ensure turbulent flow was achieved.

The PTR-MS operating conditions were held constant throughout the measurement period to ensure the reduced electric field strength (E/N , where E is the electric field strength and N is the buffer gas density) was maintained at 127 Td. The drift tube pressure, temperature and voltage were set to 2.01 mbar, 45 °C and 550 V respectively. When operating in flux mode the PTR-MS sequentially measured eight mass to charge ratios including the isotope of the primary ion (m/z 21) and first water cluster (m/z 37) which were both sampled at a rate 20 ms and m/z 33, 45, 47, 59, 61, 69 and 71 which were all sampled at 50 ms. These dwell times are much shorter than is typical when measuring VOC fluxes by PTR-MS resulting in a lower signal-to-noise ratio than might be typical. Here we only focus on the measurements of m/z 69 which we attribute entirely to isoprene. Typically the ion counts reported by the PTR-MS are converted to a meaningful concentration by first calculating the instrument sensitivity to a specific compound determined by sampling from a gas standard. During the Alice Holt campaign no gas standard was available. Consequently, the recorded ion counts of isoprene per second ($I(RH^+)$) were converted to a measurement of isoprene concentration in units of parts per billion as follows

$$[R] = \frac{1}{k\Delta t} \frac{I(RH^+)}{T(RH^+)} \left(\frac{I(H_3O^+)}{T(H_3O^+)} \right)^{-1}, \quad (1)$$

where $I(RH^+)$ and $I(H_3O^+)$ are the isoprene and primary ion counts, respectively, k is the reaction rate constant taken from Zhao and Zhang (2004) which was modified to account for the typical fragmentation of isoprene to m/z 41 under the reported operating conditions and Δt is the reaction term which is dependent upon the length of the reaction chamber. $T(RH^+)$ and $T(H_3O^+)$ are the instrument specific transmission efficiencies for isoprene and the primary ions. The transmission efficiencies were determined experimentally at the end of the measurement campaign. According to Taipale et al., (2008) the use of transmission efficiencies rather than instrument sensitivities calculated using gas standards can result in uncertainties of ~25%. The instrument background was measured once per day by sampling ambient air through a Pt/Al₂O₃ catalyst heated to 200 °C and these values were subtracted from the ambient concentration measurements. Fluxes of isoprene were calculated following the procedures outlined by Langford et al. (2009). A cross-correlation between the vertical wind velocity and isoprene concentration was calculated for each averaging period to determine the time-lag between the two datasets which arises due to the spatial separation between ultrasonic anemometer and PTR-MS. Due to the low signal-to-noise ratio of the raw isoprene data (<10), the recommendations of Langford et al. (2015) were followed to avoid systematic bias in the reported fluxes which involved the use of a prescribed time-lag which changed each day to reflect the average day-time (11:00 to 14:00) time-lag of that day.

S1.2 Ispra – Measurement setup

Isoprene flux measurements were made from June 11 to August 12, 2013 at the Ispra forest field station. The forest is further characterized with a different focus in Ferrea et al. (2012). More technical information on the general setup of the Ispra forest station can be found in Putaud et al. (2014).

5

For the turbulent flux measurements of isoprene, 10 Hz measurement data from a sonic anemometer (Gill, HS-100) were combined with 10 Hz concentration data from a fast isoprene sensor (FIS, Hills Scientific) mounted aloft a 37 m measurement tower. For the latter, air was drawn into a sampling line located 30 cm away from the sonic anemometer and carried at a flow rate of 25 slpm through a Teflon tube with 6 mm inner diameter to the FIS located inside an air conditioned container on the ground.

10

The FIS measurements are based on the detection of chemiluminescence occurring during the reaction of isoprene with ozone. Ambient air with a flow rate of 4-5 slpm and a 4 % mixture of ozone at 0.8 slpm in O₂ from an ozoniser (Hills Scientific) are mixed inside the reaction cell of the instrument. Following the reaction of isoprene with ozone, light is emitted at a characteristic wavelength and detected using single-photon counting at near-zero background. Instrument calibration to obtain isoprene concentrations was done using zero air from a gas cylinder and air with certified isoprene concentrations on a weekly basis confirming practically no drift of the zero signal and little variation in the span during the measurement campaign.

15

The covariances between the high frequency wind data and isoprene concentration data were calculated using the EdiRe software package (University of Edinburgh). The median time lag between vertical wind speed and concentration measurements was 4.7 s with little fluctuation during the measurement campaign. This value was used in the final data processing.

20

S2. Isoprene Emission Potentials

Ecosystem (E_{eco}), oak canopy (E_{can}) and leaf-level (E_{LL}) equivalent isoprene emission potentials (IEPs) and uncertainties for each of the five measurement sites are listed below. The IEPs were calculated using the six different implementations of the Guenther algorithm described in the manuscript. In each case the final IEP was determined using the weighted average IEP method.

25

S2.1 Alice Holt

Emission factors derived for Alice Holt are summarised in Tables S1 to S3.

30 **Table S1 Ecosystem-Scale isoprene emission potentials at Alice Holt**

Algorithm	E_{eco}	E_{eco+Fd}	$E_{eco+Fd+chem}$
G93	5613	6045	6347±1552
G06	6542	7046	7398±1802
PCEEA	8368	9013	9464±2296
MEGAN 2.1 (a)	9333	10052	10555±2557
MEGAN 2.1 (b)	9686	10433	10955±2653
MEGAN 2.1 (c)	8781	9458	9931±2424

Table S2 Oak canopy isoprene emission potentials at Alice Holt

Algorithm	E_{can}	E_{can+Fd}	$E_{can+Fd+chem}$
G93	6237	6717	7053±2154
G06	7269	7829	8220±2505
PCEEA	9298	10014	10515±3196
MEGAN 2.1 (a)	10370	11169	11727±3562

MEGAN 2.1 (b)	10762	11592	12172±3695
MEGAN 2.1 (c)	9757	10509	11034±3352

Table S3 Leaf-level equivalent isoprene emission potentials at Alice Holt

Algorithm	E_{LL}	E_{LL+Fd}	$E_{LL+Fd+chem}$
G93	74	80	84±31
G06	77	83	87±32
PCEEA	98	106	111±41
MEGAN 2.1 (a)	110	118	124±46
MEGAN 2.1 (b)	114	123	129±47
MEGAN 2.1 (c)	103	111	117±43

S2.1 Bosco Fontana

5 Emission factors derived for Bosco Fontana are summarised in Tables S4 to S6.

Table S4 Ecosystem-Scale isoprene emission potentials at Bosco Fontana

Algorithm	E_{eco}	E_{eco+Fd}	$E_{eco+Fd+chem}$
G93	1529	1722	1791±440
G06	720	810	843±375
PCEEA	1488	1675	1742±441
MEGAN 2.1 (a)	1376	1550	1612±428
MEGAN 2.1 (b)	1338	1507	1578±424
MEGAN 2.1 (c)	1980	2230	2319±493

Table S5 Oak canopy isoprene emission potentials at Bosco Fontana

Algorithm	E_{can}	E_{can+Fd}	$E_{can+Fd+chem}$
G93	5663	6378	6633±4002
G06	2667	3000	3120±2212
PCEEA	5511	6204	6452±3906
MEGAN 2.1 (a)	5096	5741	5970±3648
MEGAN 2.1 (b)	4956	5581	5805±3560
MEGAN 2.1 (c)	7333	8259	8590±5069

10 **Table S6 Leaf-level equivalent isoprene emission potentials at Bosco Fontana**

Algorithm	E_{LL}	E_{LL+Fd}	$E_{LL+Fd+chem}$
G93	66	74	77±49
G06	28	31	32±25
PCEEA	58	65	68±46
MEGAN 2.1 (a)	54	61	63±43
MEGAN 2.1 (b)	52	59	61±42
MEGAN 2.1 (c)	77	87	91±60

S2.3 Castelporziano

Emission factors derived for Bosco Fontana are summarised in Tables S7 to S9.

Table S7 Ecosystem-Scale isoprene emission potentials at Castelporziano

Algorithm	E_{eco}	E_{eco+Fd}	$E_{eco+Fd+chem}$
G93	99	106	111±14
G06	66	70	74±11
PCEEA	122	130	137±16
MEGAN 2.1 (a)	107	115	121±15
MEGAN 2.1 (b)	110	117	123±14
MEGAN 2.1 (c)	144	155	163±19

Table S8 Oak canopy isoprene emission potentials at Castelporziano

Algorithm	E_{can}	E_{can+Fd}	$E_{can+Fd+chem}$
G93	360	385	405±232
G06	240	255	267±156
PCEEA	444	473	496±285
MEGAN 2.1 (a)	389	418	439±251
MEGAN 2.1 (b)	400	425	447±257
MEGAN 2.1 (c)	524	564	592±337

Table S9 Leaf-level equivalent isoprene emission potentials at Castelporziano

Algorithm	E_{LL}	E_{LL+Fd}	$E_{LL+Fd+chem}$
G93	2.1	2.3	2.4±1.4
G06	1.2	1.3	1.4±0.9
PCEEA	2.3	2.4	2.5±1.7
MEGAN 2.1 (a)	2.0	2.1	2.2±1.5
MEGAN 2.1 (b)	2.0	2.2	2.3±1.5
MEGAN 2.1 (c)	2.7	2.9	3.0±2.0

S2.4 Ispra

Emission factors derived for Ispra are summarised in Tables S10 to S12.

Table S10 Ecosystem-Scale isoprene emission potentials at Ispra

Algorithm	E_{eco}	E_{eco+Fd}	$E_{eco+Fd+chem}$
G93	5824	6385	6704±983
G06	3591	3937	4133±748
PCEEA	6975	7646	8029±1120
MEGAN 2.1 (a)	6599	7234	7596±1074
MEGAN 2.1 (b)	6670	7312	7678±1082
MEGAN 2.1 (c)	8598	9426	9897±1321

Table S11 Oak canopy isoprene emission potentials at Ispra

Algorithm	E_{can}	E_{can+Fd}	$E_{can+Fd+chem}$
G93	7281	7981	8380±2073
G06	4489	4921	5167±1391
PCEEA	8719	9558	10036±2443
MEGAN 2.1 (a)	8249	9042	9495±2321
MEGAN 2.1 (b)	8338	9140	9597±2344
MEGAN 2.1 (c)	10748	11782	12371±2969

Table S12 Leaf-level equivalent isoprene emission potentials at Ispra

Algorithm	E_{LL}	E_{LL+Fd}	$E_{LL+Fd+chem}$
G93	74	81	85±27
G06	40	44	46±16
PCEEA	76	84	88±28
MEGAN 2.1 (a)	72	79	83±27
MEGAN 2.1 (b)	73	80	84±27
MEGAN 2.1 (c)	94	103	108±35

S2.4 O3HP

Emission factors derived for O3HP are summarised in Tables S13 to S15.

Table S13 Ecosystem-Scale isoprene emission potentials at O3HP

Algorithm	E_{eco}	E_{eco+Fd}	$E_{eco+Fd+chem}$
G93	5135	5642	5924±771
G06	3439	3779	3967±551
PCEEA	7018	7710	8096±1026
MEGAN 2.1 (a)	6926	7610	7990±1014
MEGAN 2.1 (b)	7606	8357	8775±1107
MEGAN 2.1 (c)	8684	9541	10018±1255

Table S14 Oak canopy isoprene emission potentials at O3HP

Algorithm	E_{can}	E_{can+Fd}	$E_{can+Fd+chem}$
G93	6847	7523	7899±1945
G06	4586	5038	5290±1328
PCEEA	9357	10280	10794±2639
MEGAN 2.1 (a)	9235	10146	10654±2605
MEGAN 2.1 (b)	10142	11142	11699±2857
MEGAN 2.1 (c)	11579	12721	13357±3256

Table S15 Leaf-level equivalent isoprene emission potentials at O3HP

Algorithm	E_{LL}	E_{LL+Fd}	$E_{LL+Fd+chem}$
G93	68	74	78±25
G06	40	44	47±15
PCEEA	58	64	67±24
MEGAN 2.1 (a)	57	63	66±24
MEGAN 2.1 (b)	63	69	73±26
MEGAN 2.1 (c)	72	79	83±29

S3 Comparison of isoprene emission potentials

Tables S16 to S25 show a comparison of IEPs calculated at each of the five measurement sites using seven different methods to derive the average isoprene emission potential. All emission potentials shown have been corrected for deposition and chemical losses. The data in these tables forms the basis of Fig. 3 in the main manuscript.

S3.1 Alice Holt, UK

Table S16 Comparison of isoprene emission potentials calculated using the MEGAN 2.1 (a) emission algorithm for Alice Holt in conjunction with the least square regression, orthogonal distance regression, weighted average and several variations of the midday average methods.

	Fluxes	\overline{IEP} (weighted)	\overline{IEP} (all hours)	\overline{IEP} (08 to 18)	\overline{IEP} (10 to 15)	\overline{IEP} (11 to 13)	LSR	ODR
IEP [$\mu\text{g m}^{-2} \text{h}^{-1}$]	-	10555	13251	11712	12316	12671	9349	12217
Mean [$\mu\text{g m}^{-2} \text{h}^{-1}$]	779	779	978	864	909	935	690	902
σ [$\mu\text{g m}^{-2} \text{h}^{-1}$]	1066	1097	1378	1218	1281	1317	972	1270
r^2	-	0.54	0.54	0.54	0.54	0.54	0.54	0.54
M score	-	1.37	1.34	1.31	1.31	1.32	1.53	1.31

Relative Bias [%]	-	0	26	11	17	20	-11	16
-------------------	---	---	----	----	----	----	-----	----

Table S17 Comparison of isoprene emission potentials calculated using the G93 emission algorithm for Alice Holt in conjunction with the least square regression, orthogonal distance regression, weighted average and several variations of the midday average methods.

	Fluxes	\overline{IEP} (weighted)	\overline{IEP} (all hours)	\overline{IEP} (08 to 18)	\overline{IEP} (10 to 15)	\overline{IEP} (11 to 13)	LSR	ODR
IEP [$\mu\text{g m}^{-2} \text{h}^{-1}$]	-	6348	6062	6261	7607	8344	6995	7538
Mean [$\mu\text{g m}^{-2} \text{h}^{-1}$]	779	779	744	768	933	1024	858	925
σ [$\mu\text{g m}^{-2} \text{h}^{-1}$]	1327	915	874	902	1096	1203	1008	1086
r^2	0.58	0.58	0.58	0.58	0.58	0.58	0.58	0.58
M score	-	1.239	1.315	1.260	1.065	1.054	1.121	1.069
Relative Bias [%]	-	0	-4	-1	20	31	10	19

S3.2 Bosco Fontana, Italy

Table S18 Comparison of isoprene emission potentials calculated using the MEGAN 2.1 (a) emission algorithm for Bosco Fontana in conjunction with the least square regression, orthogonal distance regression, weighted average and several variations of the midday average methods.

	Fluxes	\overline{IEP} (weighted)	\overline{IEP} (all hours)	\overline{IEP} (08 to 18)	\overline{IEP} (10 to 15)	\overline{IEP} (11 to 13)	LSR	ODR
IEP [$\mu\text{g m}^{-2} \text{h}^{-1}$]	-	1550	1493	1647	1509	1527	1489	1547
Mean [$\mu\text{g m}^{-2} \text{h}^{-1}$]	862	862	830	916	839	849	828	860
σ [$\mu\text{g m}^{-2} \text{h}^{-1}$]	1113	1053	1015	1119	1026	1038	1012	1052
r^2	-	0.79	0.79	0.79	0.79	0.79	0.79	0.79
M score	-	0.347	0.356	0.347	0.353	0.350	0.357	0.347
Relative Bias [%]	-	0	-4	6	-3	-1	-4	0

Table S19 Comparison of isoprene emission potentials calculated using the G93 emission algorithm for Bosco Fontana in conjunction with the least square regression, orthogonal distance regression, weighted average and several variations of the midday average methods.

	Fluxes	\overline{IEP} (weighted)	\overline{IEP} (all hours)	\overline{IEP} (08 to 18)	\overline{IEP} (10 to 15)	\overline{IEP} (11 to 13)	LSR	ODR
IEP [$\mu\text{g m}^{-2} \text{h}^{-1}$]	-	1722	1229	1643	1996	2240	1953	1495
Mean [$\mu\text{g m}^{-2} \text{h}^{-1}$]	862	862	615	822	999	1121	977	748
σ [$\mu\text{g m}^{-2} \text{h}^{-1}$]	1113	854	609	815	990	1111	968	741
r^2	-	0.75	0.75	0.75	0.75	0.75	0.75	0.75
M score	-	0.66	1.17	0.70	0.59	0.61	0.60	0.81
Relative Bias [%]	-	0	-29	-5	16	30	13	-13

S3.3 Castelporziano, Italy

Table S20 Comparison of isoprene emission potentials calculated using the MEGAN 2.1 (a) emission algorithm for Castelporziano in conjunction with the least square regression, orthogonal distance regression, weighted average and several variations of the midday average methods.

	Fluxes	\overline{IEP} (weighted)	\overline{IEP} (all hours)	\overline{IEP} (08 to 18)	\overline{IEP} (10 to 15)	\overline{IEP} (11 to 13)	LSR	ODR
IEP [$\mu\text{g m}^{-2} \text{h}^{-1}$]	-	74	80	80	72	74	71	82
Mean [$\mu\text{g m}^{-2} \text{h}^{-1}$]	44	44	48	48	44	44	43	49
σ [$\mu\text{g m}^{-2} \text{h}^{-1}$]	70	57	61	61	56	56	54	63
r^2	-	0.54	0.54	0.54	0.54	0.54	0.54	0.54
M score	-	1.26	1.19	1.19	1.28	1.28	1.31	1.18
Relative Bias [%]	-	0	8	8	-2	0	-4	11

Table S21 Comparison of isoprene emission potentials calculated using the G93 emission algorithm for Castelporziano in conjunction with the least square regression, orthogonal distance regression, weighted average and several variations of the midday average methods.

	Fluxes	\overline{IEP} (weighted)	\overline{IEP} (all hours)	\overline{IEP} (08 to 18)	\overline{IEP} (10 to 15)	\overline{IEP} (11 to 13)	LSR	ODR
IEP [$\mu\text{g m}^{-2} \text{h}^{-1}$]	-	112	105	113	118	133	119	117
Mean [$\mu\text{g m}^{-2} \text{h}^{-1}$]	44	44	42	45	47	53	48	47
σ [$\mu\text{g m}^{-2} \text{h}^{-1}$]	70	48	45	49	51	57	51	50
r^2	-	0.49	0.49	0.49	0.49	0.49	0.49	0.49
M score	-	1.41	1.51	1.39	1.33	1.22	1.30	1.34
Relative Bias [%]	-	0	-5	2	6	19	7	5

S3.4 Ispra, Italy

Table S22 Comparison of isoprene emission potentials calculated using the MEGAN 2.1 (a) emission algorithm for Ispra in conjunction with the least square regression, orthogonal distance regression, weighted average and several variations of the midday average methods.

	Fluxes	\overline{IEP} (weighted)	\overline{IEP} (all hours)	\overline{IEP} (08 to 18)	\overline{IEP} (10 to 15)	\overline{IEP} (11 to 13)	LSR	ODR
IEP [$\mu\text{g m}^{-2} \text{h}^{-1}$]	-	7596	7212	7558	7928	8142	7504	9174
Mean [$\mu\text{g m}^{-2} \text{h}^{-1}$]	2108	2108	2002	2098	2201	2261	2083	2546
σ [$\mu\text{g m}^{-2} \text{h}^{-1}$]	3126	2940	2792	2925	3069	3152	2905	3551
r^2	-	0.86	0.86	0.86	0.86	0.86	0.86	0.86
M score	-	0.28	0.32	0.29	0.27	0.27	0.29	0.31
Relative Bias [%]	-	0	-5	0	4	7	-1	21

Table S23 Comparison of isoprene emission potentials calculated using the G93 emission algorithm for Ispra in conjunction with the least square regression, orthogonal distance regression, weighted average and several variations of the midday average methods.

Fluxes	\overline{IEP} (weighted)	\overline{IEP} (all hours)	\overline{IEP} (08 to 18)	\overline{IEP} (10 to 15)	\overline{IEP} (11 to 13)	LSR	ODR
--------	--------------------------------	---------------------------------	--------------------------------	--------------------------------	--------------------------------	-----	-----

IEP [$\mu\text{g m}^{-2} \text{h}^{-1}$]	-	6703	5969	7629	7733	8359	7512	6966
Mean [$\mu\text{g m}^{-2} \text{h}^{-1}$]	2108	2108	1877	2399	2432	2629	2363	2190
σ [$\mu\text{g m}^{-2} \text{h}^{-1}$]	3126	2401	2139	2733	2771	2995	2691	2496
r^2	-	0.78	0.78	0.78	0.78	0.78	0.78	0.78
M score	-	0.51	0.65	0.44	0.43	0.44	0.44	0.48
Relative Bias [%]	-	0	-11	14	15	25	12	4

S3.5 O3HP, France

5

Table S24 Comparison of isoprene emission potentials calculated using the MEGAN 2.1 (a) emission algorithm for O3HP in conjunction with the least square regression, orthogonal distance regression, weighted average and several variations of the midday average methods.

	Fluxes	\overline{IEP} (weighted)	\overline{IEP} (all hours)	\overline{IEP} (08 to 18)	\overline{IEP} (10 to 15)	\overline{IEP} (11 to 13)	LSR	ODR
IEP [$\mu\text{g m}^{-2} \text{h}^{-1}$]		7991	6914	7795	7883	7889	8138	8018
Mean [$\mu\text{g m}^{-2} \text{h}^{-1}$]	899	899	777	877	886	887	915	902
σ [$\mu\text{g m}^{-2} \text{h}^{-1}$]	1371	1279	1107	1247	1262	1262	1302	1283
r^2	-	0.90	0.90	0.90	0.90	0.90	0.90	0.90
M score	-	0.23	0.34	0.24	0.23	0.23	0.22	0.23
Relative Bias [%]	-	0	0	-13	-2	-1	0	2

10

Table S25 Comparison of isoprene emission potentials calculated using the G93 emission algorithm for O3HP in conjunction with the least square regression, orthogonal distance regression, weighted average and several variations of the midday average methods.

	Fluxes	\overline{IEP} (weighted)	\overline{IEP} (all hours)	\overline{IEP} (08 to 18)	\overline{IEP} (10 to 15)	\overline{IEP} (11 to 13)	LSR	ODR
IEP [$\mu\text{g m}^{-2} \text{h}^{-1}$]		5924	6894	5607	6576	6902	7225	5513
Mean [$\mu\text{g m}^{-2} \text{h}^{-1}$]	899	899	1046	851	998	1047	1096	836
σ [$\mu\text{g m}^{-2} \text{h}^{-1}$]	1371	1031	1200	977	1145	1201	1258	960
r^2	-	0.84	0.84	0.84	0.84	0.84	0.84	0.84
M score	-	0.43	0.34	0.49	0.36	0.34	0.34	0.52
Relative Bias [%]	-	0	16	-5	11	16	22	-7

15

20

5

10

Figures S1 to S4 show the average diurnal profile of the isoprene emission potential that have been calculated by inverting the G93 (Panel A) and MEGAN 2.1 (a) (Panel C) emission algorithms. Also shown are the average emission potential assigned to each site which were calculated using seven different methods (see main text for details).

S4.1 Alice Holt

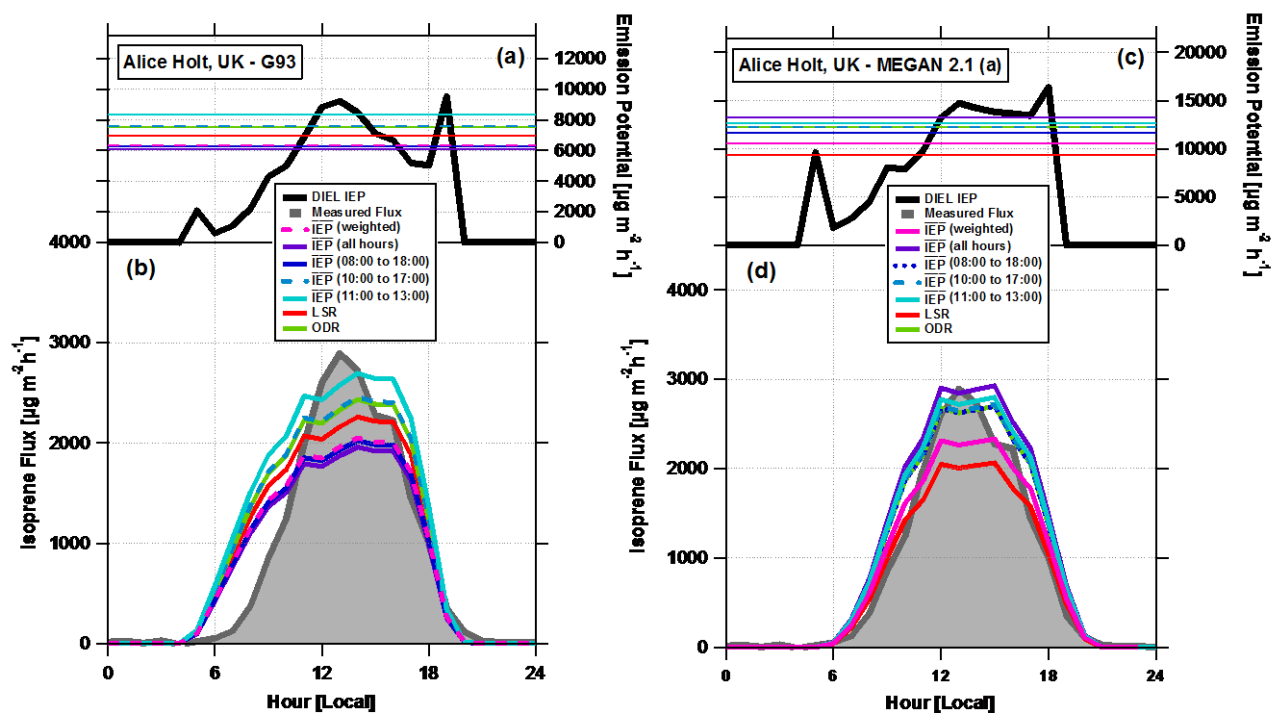


Figure S1 Panels A and C show the average diurnal cycle in the isoprene emission potential (e.g. $IEP = \left(\frac{F_{iso}}{\gamma} \right)$) calculated for the Alice Holt site, UK using the G93 (panel A) and MEGAN 2.1 (panel B) algorithms. Superimposed on top of these are the isoprene emission potentials calculated using the least square regression, orthogonal distance regression and average (with several averaging lengths) methods – see text for detailed description. Panels B and D show the average diurnal cycle of the measured fluxes and the average diurnal cycle of the fluxes modelled using the seven different isoprene emission potentials calculated for this data set.

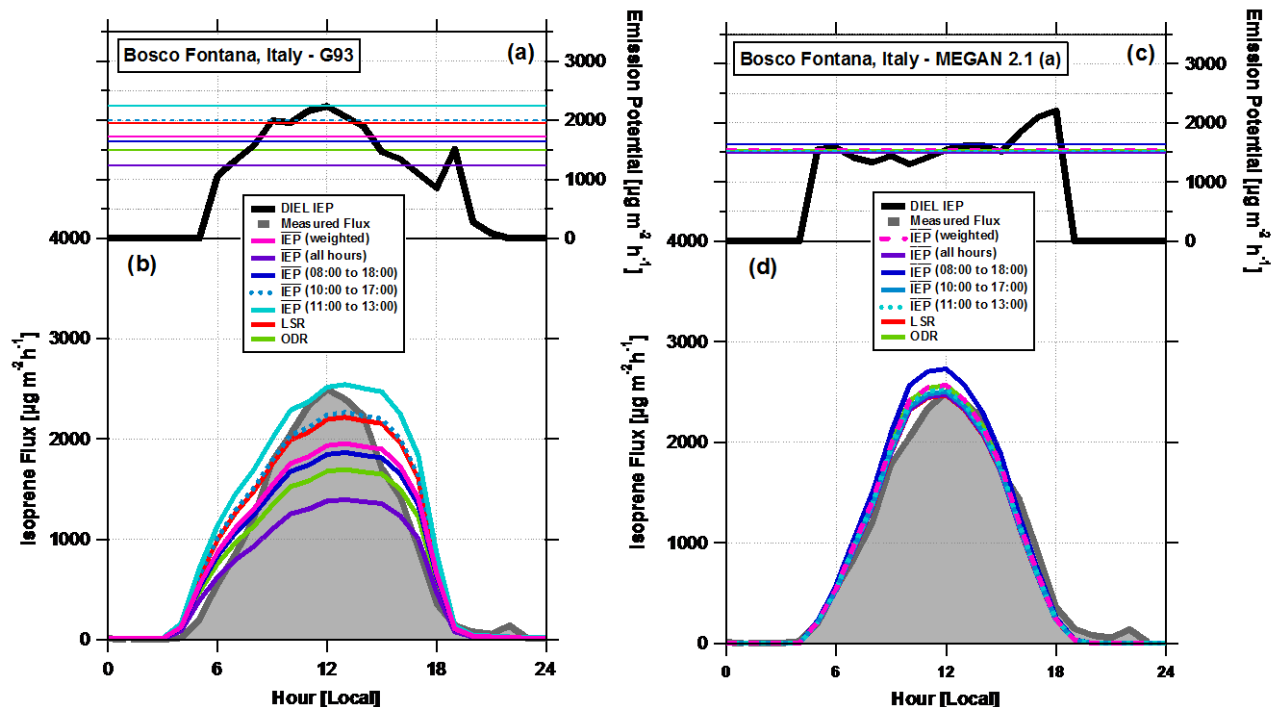


Figure S2 Panels A and C show the average diurnal cycle in the isoprene emission potential (e.g. $IEP = \left(\frac{F_{iso}}{\gamma} \right)$) calculated for the Bosco Fontana site, Italy using the G93 (panel A) and MEGAN 2.1 (panel B) algorithms. Superimposed on top of these are the isoprene emission potentials calculated using the least square regression, orthogonal distance regression and average (with several averaging lengths) methods – see text for detailed description. Panels B and D show the average diurnal cycle of the measured fluxes and the average diurnal cycle of the fluxes modelled using the seven different isoprene emission potentials calculated for this data set.

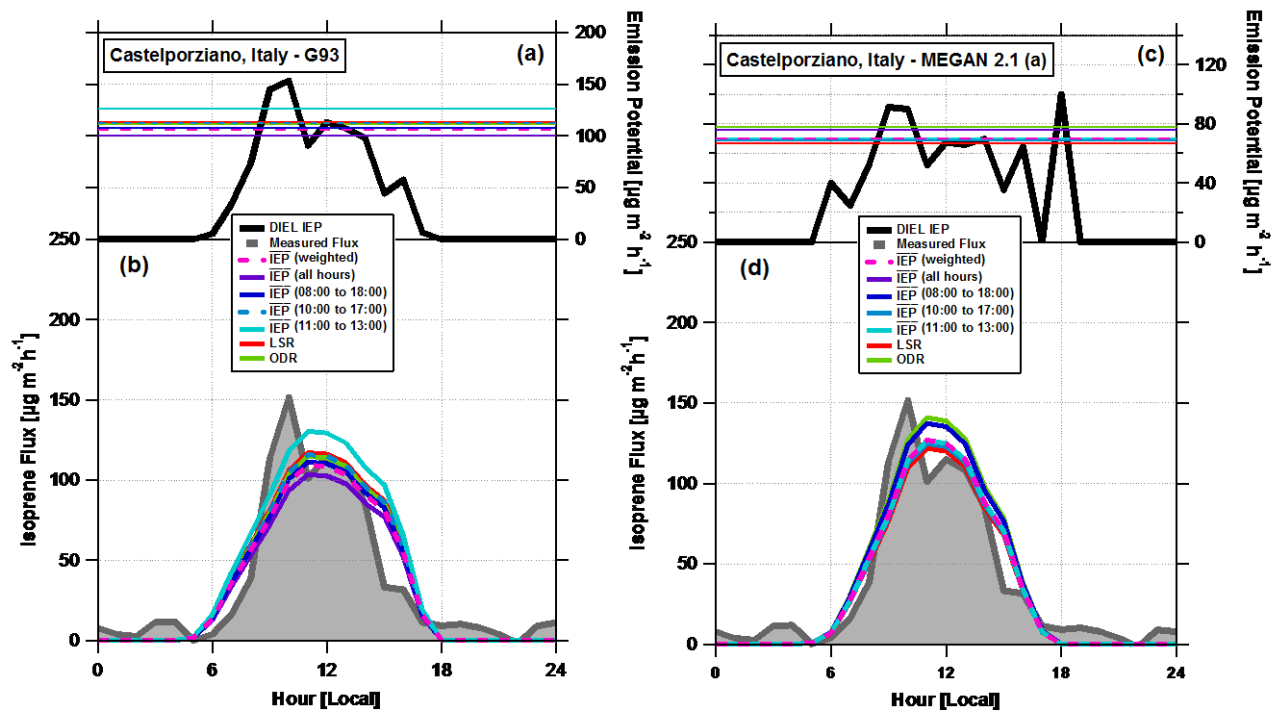


Figure S3 Panels A and C show the average diurnal cycle in the isoprene emission potential (e.g. $IEP = \left(\frac{F_{iso}}{\gamma} \right)$) calculated for the Castelporziano site, Italy using the G93 (panel A) and MEGAN 2.1 (panel B) algorithms. Superimposed on top of these are the isoprene emission potentials calculated using the least square regression, orthogonal distance regression and average (with several averaging lengths) methods – see text for detailed description. Panels B and D show the average diurnal cycle of the measured fluxes and the average diurnal cycle of the fluxes modelled using the seven different isoprene emission potentials calculated for this data set.

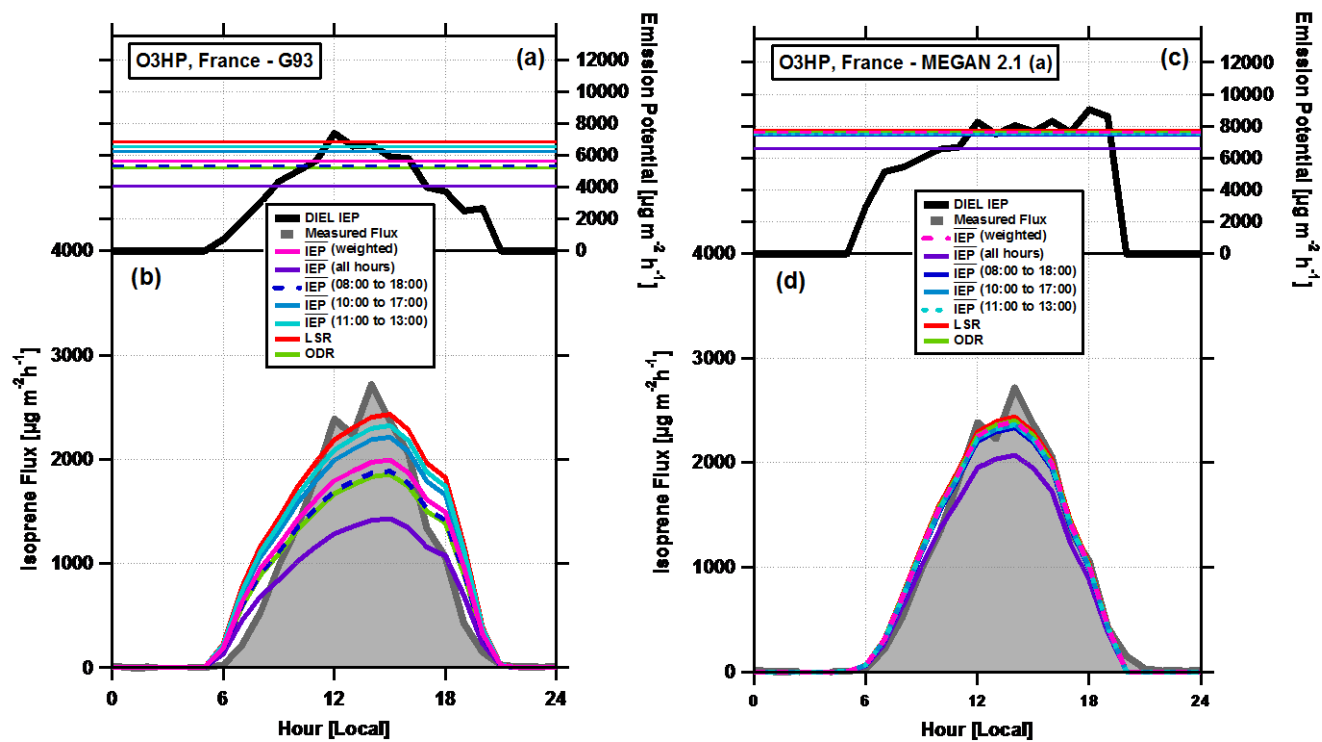


Figure S4 Panels A and C show the average diurnal cycle in the isoprene emission potential (e.g. $IEP = \left(\frac{F_{Iso}}{\gamma} \right)$) calculated for the Observatoire de Haute Provence site, France using the G93 (panel A) and MEGAN 2.1 (panel B) algorithms. Superimposed on top of these are the isoprene emission potentials calculated using the least square regression, orthogonal distance regression and average (with several averaging lengths) methods – see text for detailed description. Panels B and D show the average diurnal cycle of the measured fluxes and the average diurnal cycle of the fluxes modelled using the seven different isoprene emission potentials calculated for this data set.

S5 Influence of past light and temperature on calculated emission potential

Within the MEGAN model the influence of past light and temperature on derived emission potentials is considered relative to a set of standard within canopy, leaf-level, conditions. When experimentalists use the MEGAN model in a big-leaf approach, these leaf-level conditions are typically calculated using measurements of PPFD and temperature made above the forest canopy. Figures S5 to S9 show the time series of the average 24 hour and 240 hour above canopy PPFD and temperature for each of the five sites relative to the leaf-level standard conditions used in MEGAN. Typically the past 24 and 240 hour PPFD is considerably higher than the standard conditions which results in a much larger gamma factor and a reduced emission potential. For this reason, it is our recommendation that the MEGAN model should not be used to derive emission potentials unless coupled to an appropriate canopy environment model.

S5.1 Alice Holt

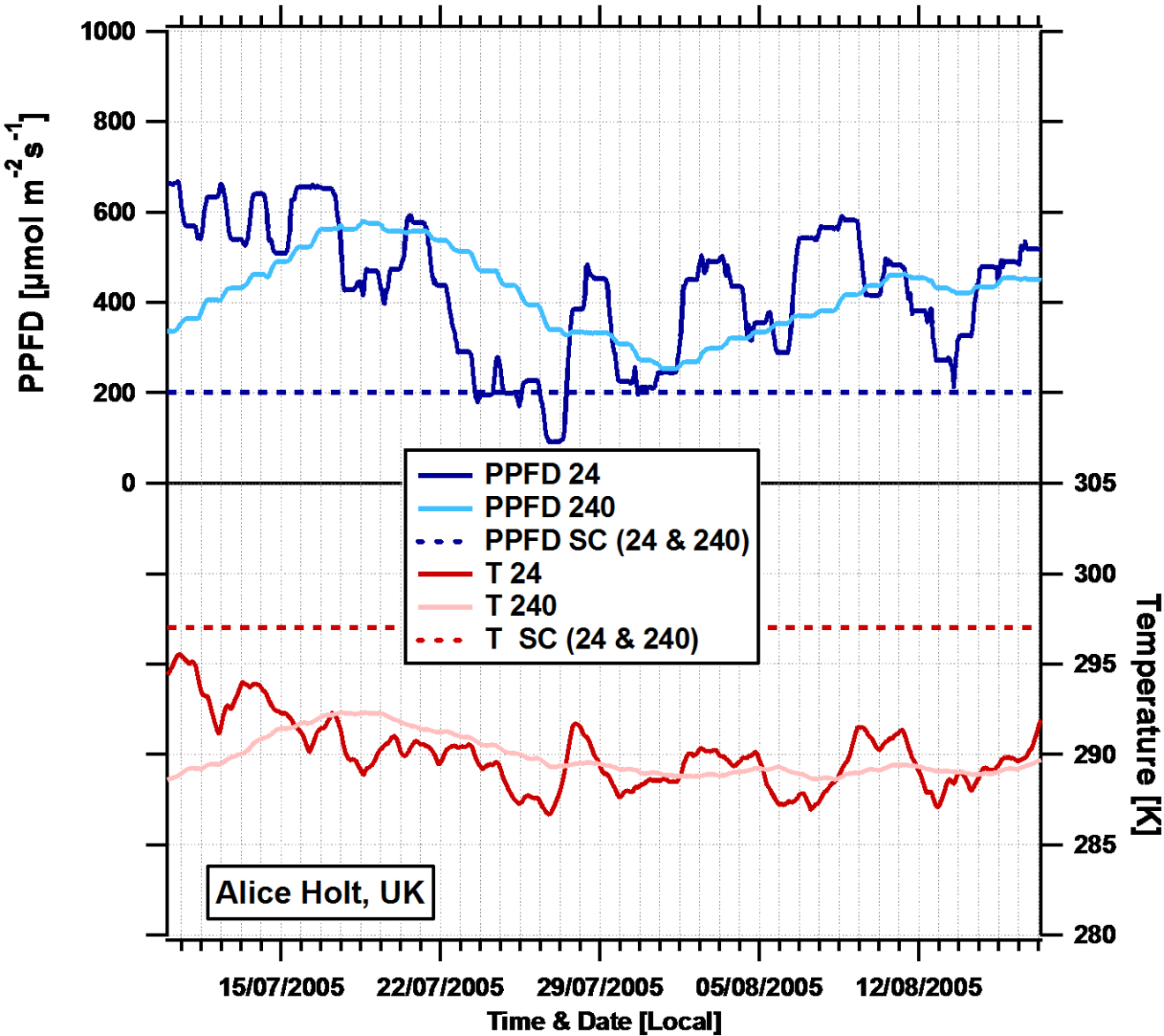
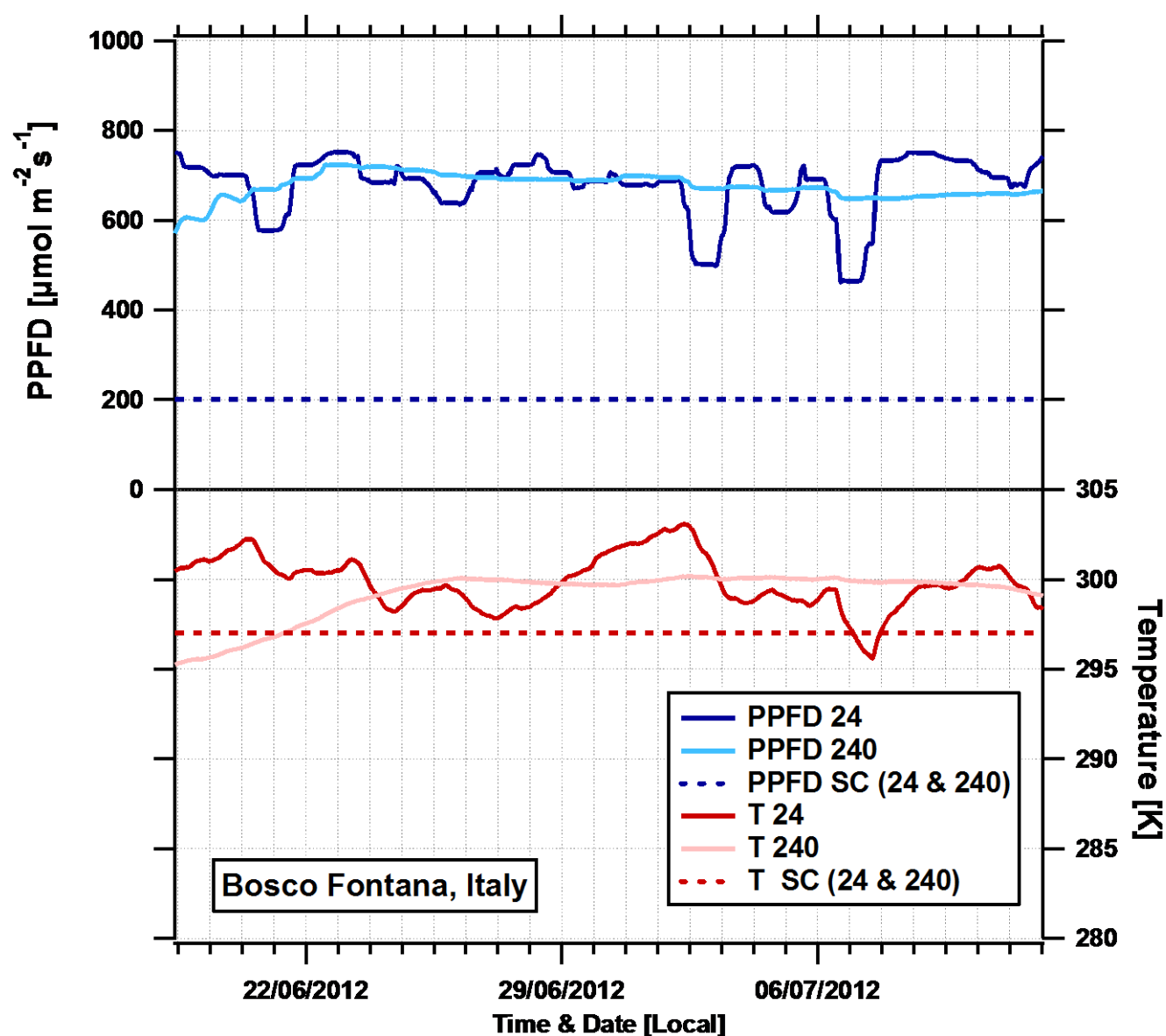


Figure S5. Time series of the previous (24 and 240 hours) above canopy light and temperature measurements made at the Alice Holt site relative to the standard conditions used in the Model of Emission of Gases and Aerosols from Nature (dashed lines) for leaf-level canopy average temperature and light.



5 Figure S6. Time series of the previous (24 and 240 hours) above canopy light and temperature measurements made at the Bosco Fontana site relative to the standard conditions used in the Model of Emission of Gases and Aerosols from Nature (dashed lines) for leaf-level canopy average temperature and light.

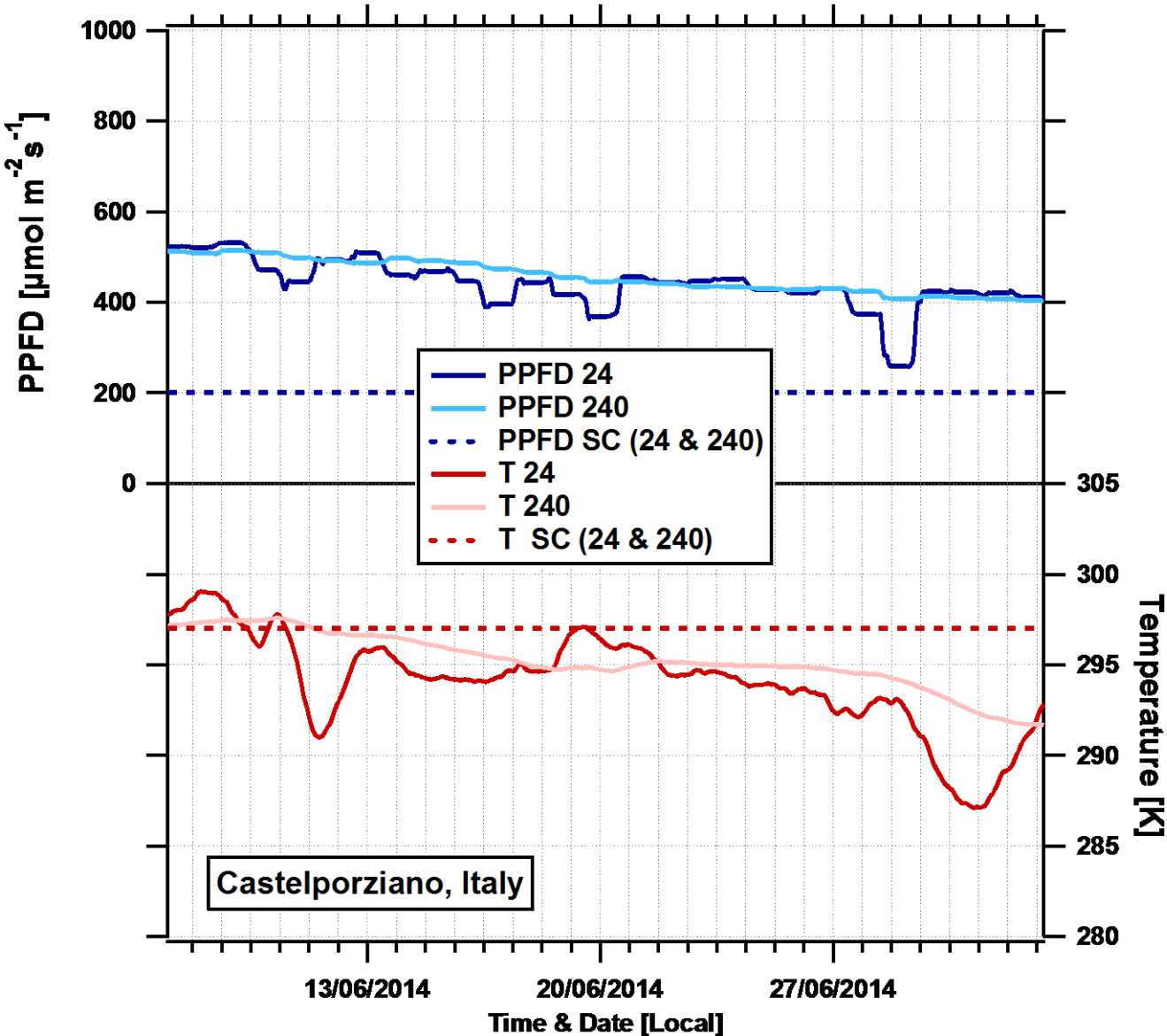


Figure S7. Time series of the previous (24 and 240 hours) above canopy light and temperature measurements made at the Castelporziano site relative to the standard conditions used in the Model of Emission of Gases and Aerosols from Nature (dashed lines) for leaf-level canopy average temperature and light.

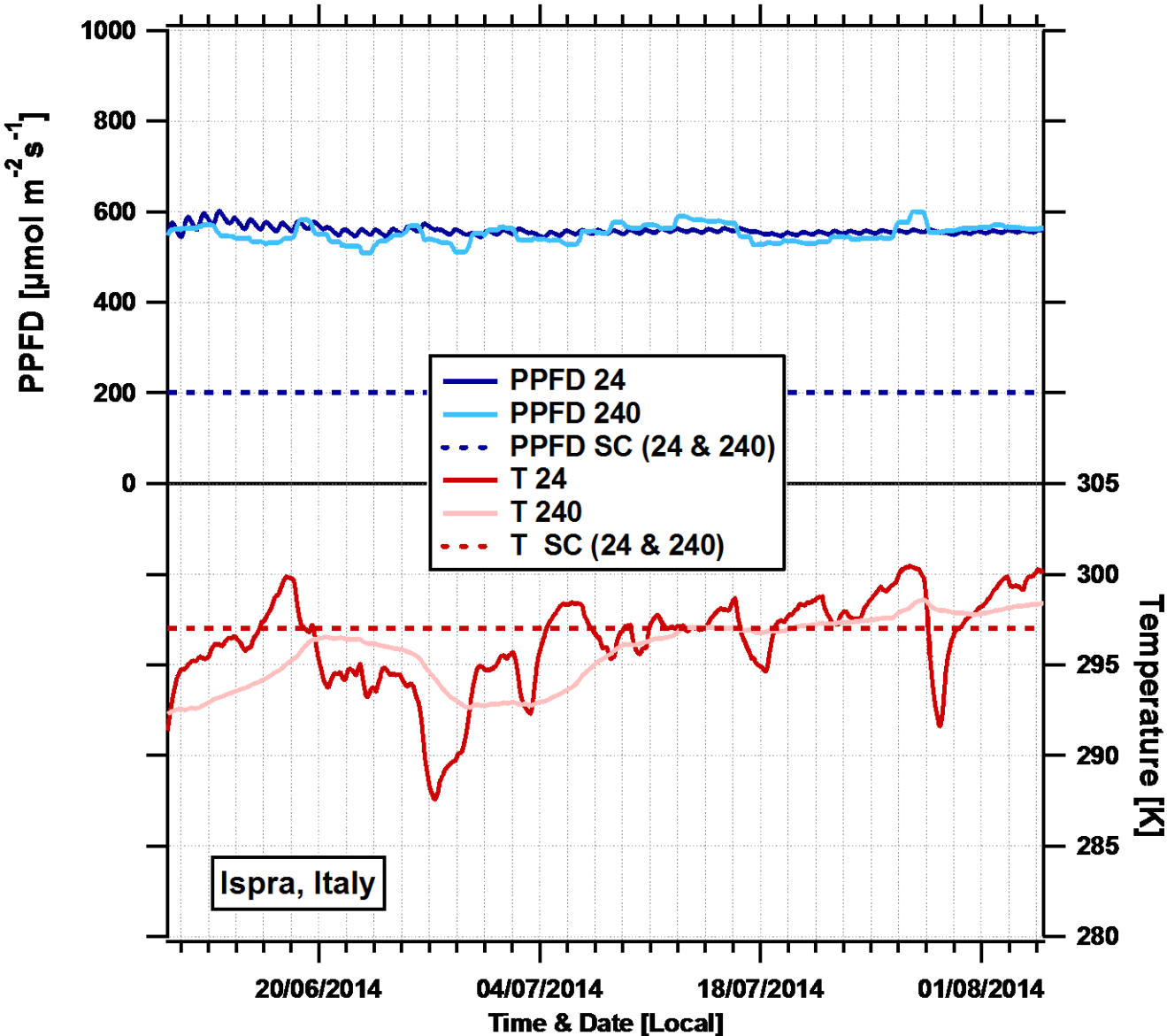
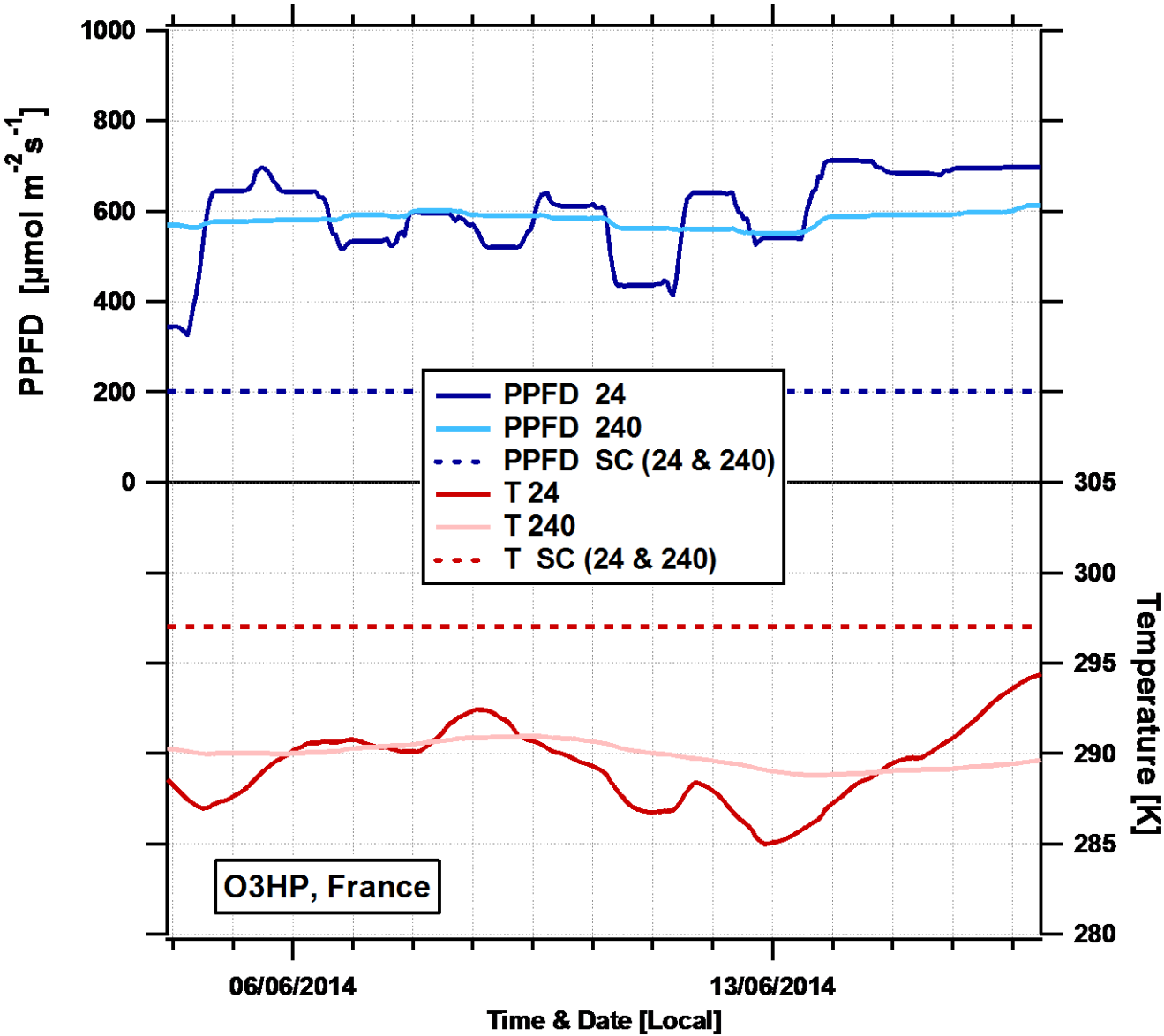


Figure S8. Time series of the previous (24 and 240 hours) above canopy light and temperature measurements made at the Ispra forest site relative to the standard conditions used in the Model of Emission of Gases and Aerosols from Nature (dashed lines) for leaf-level canopy average temperature and light.



5 Figure S9. Time series of the previous (24 and 240 hours) above canopy light and temperature measurements made at the Observatoire de Haute Provence site relative to the standard conditions used in the Model of Emission of Gases and Aerosols from Nature (dashed lines) for leaf-level canopy average temperature and light.

S6 Species composition uncertainty

10 Species composition data for each of the five measurement sites was available, but no uncertainties were stated. Here, we attempt to assess the uncertainty by performing wind rose analysis of the isoprene emission potentials to assess how they vary spatially. Figure S10 shows the isoprene emission potential wind rose (red) for the Alice Holt, Bosco Fontana and Ispra forest sites relative to the average isoprene emission potential (blue). This analysis showed the spatial variation to range from 14% at Alice Holt to 28% at Bosco Fontana. For the remaining two sites, Castelporziano and O3HP, where there was insufficient
15 data to perform a detailed wind rose analysis, uncertainties of 20% were assigned.

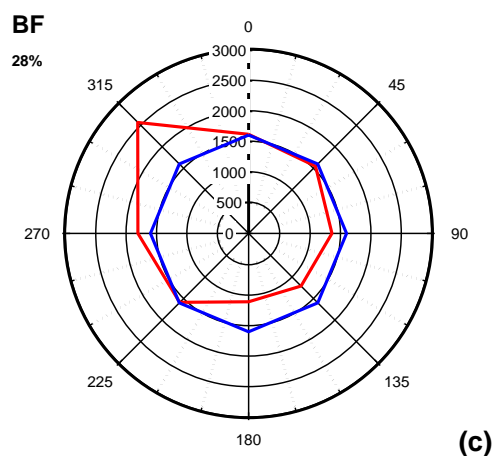
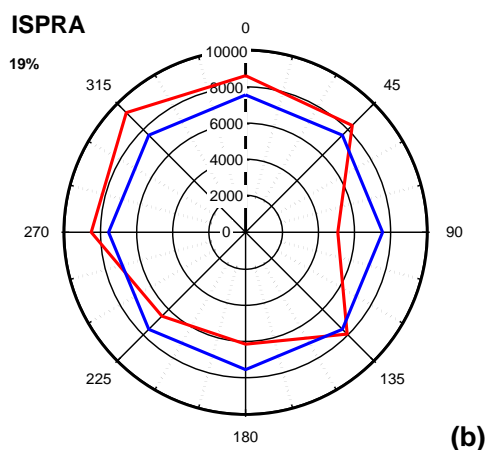
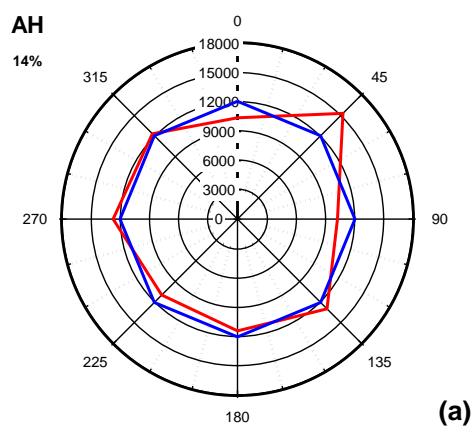


Figure S10 Calculated isoprene emission potential by wind sector (red) and site average (blue) for the Alice Holt (a), Ispra (b) and Bosco Fontana (c) measurement sites.

S7 Reporting fluxes for a set of defined conditions

Above canopy flux measurements may be used to determine an emission potential for a specific set of defined conditions. We used two-dimensional histograms to determine the most common set of light and temperature conditions observed during day time at each of the five measurement sites. The histograms binned the number of flux averaging periods that corresponded to specific bin ranges of light ($\pm 200 \mu\text{mol m}^{-2} \text{s}^{-1}$) and temperature ($\pm 1 \text{ K}$). The results for the are shown in figures S11 to S14

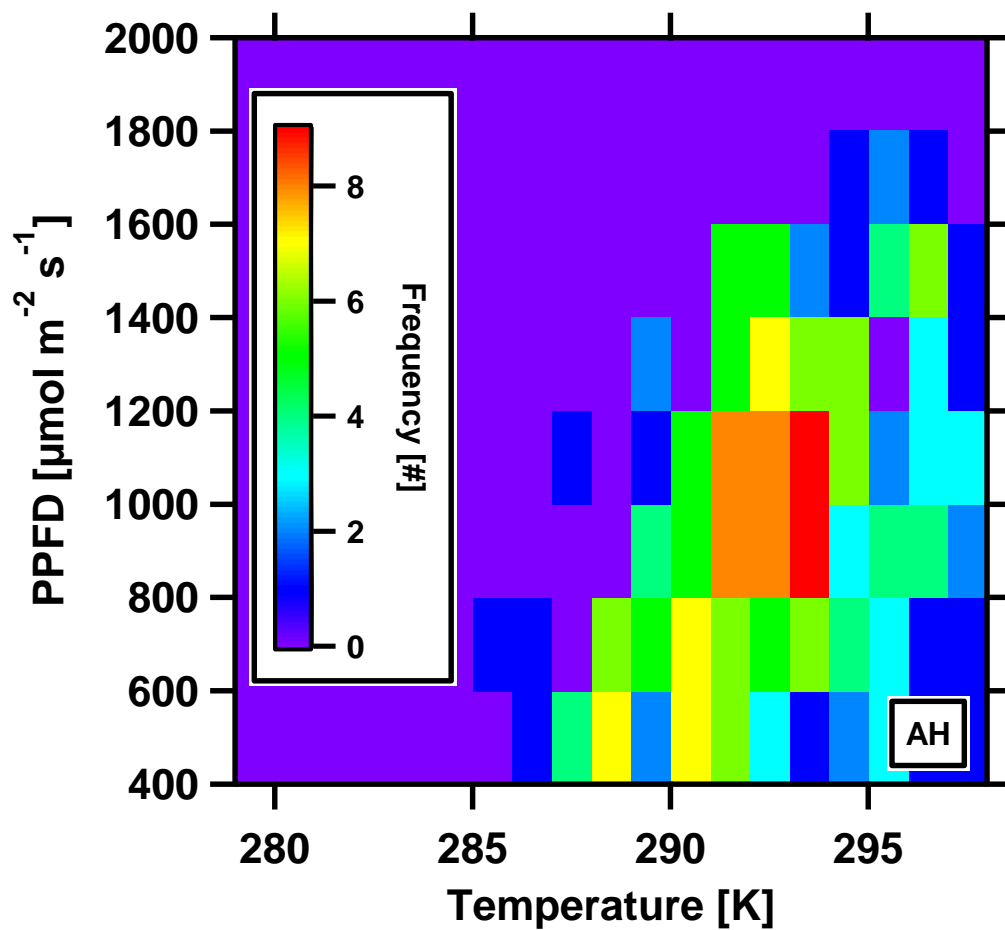


Figure S11 Two dimensional histogram plot of flux averaging periods that correspond to bins of light ($\pm 200 \mu\text{mol m}^{-2} \text{s}^{-1}$) and temperature ($\pm 1 \text{ K}$) at the Alice Holt measurement site.

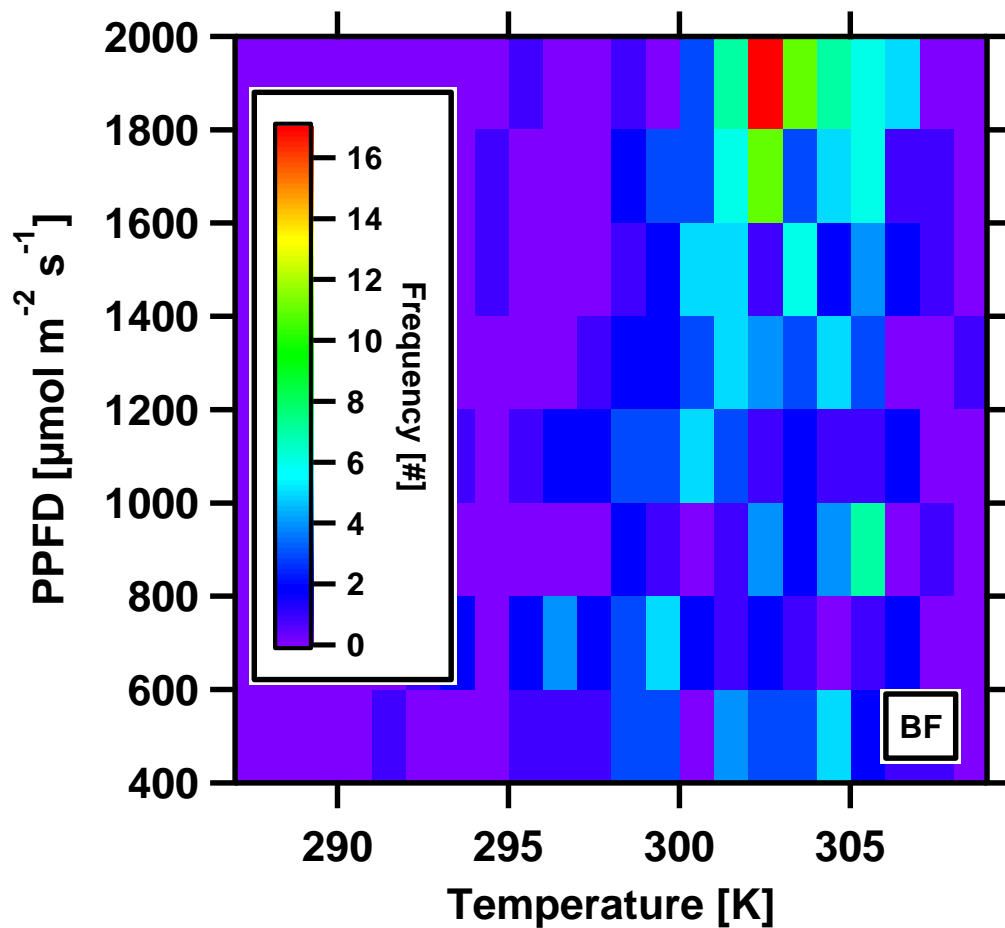


Figure S12 Two dimensional histogram plot of flux averaging periods that correspond to bins of light ($\pm 200 \mu\text{mol m}^{-2} \text{s}^{-1}$) and temperature ($\pm 1 \text{ K}$) at the Bosco Fontana measurement site.

5

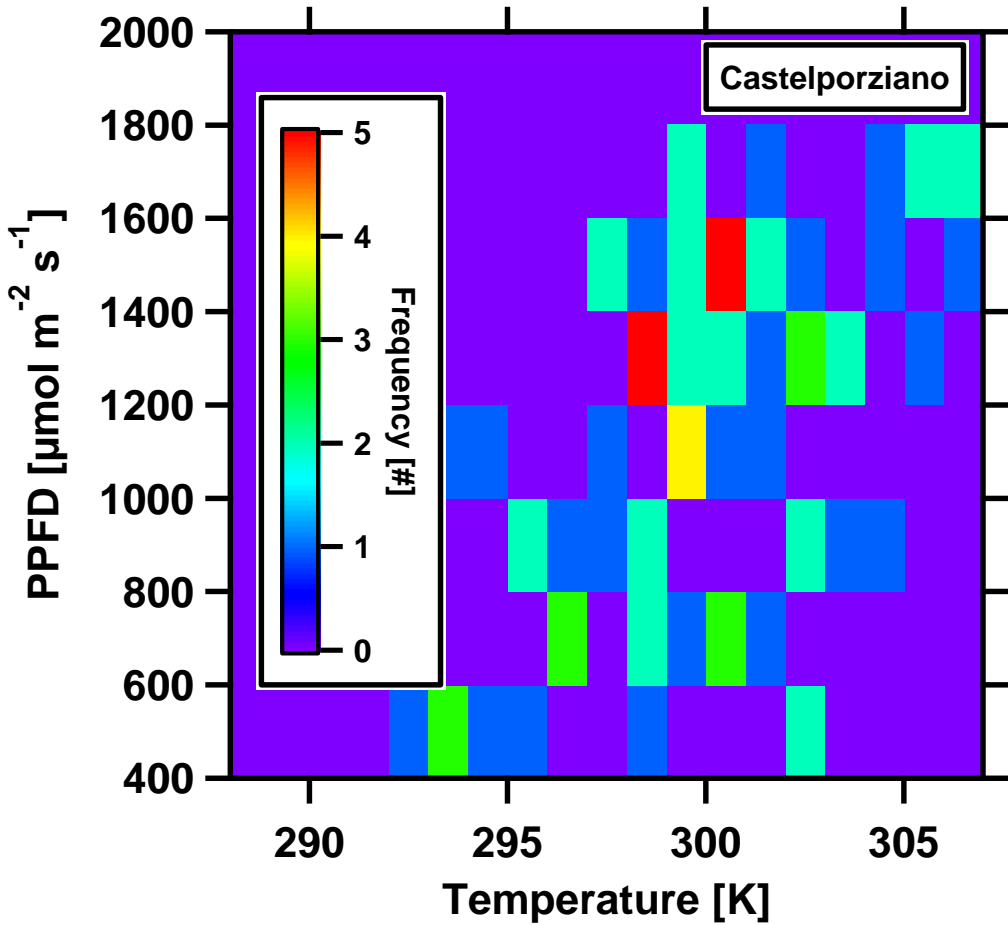


Figure S13 Two dimensional histogram plot of flux averaging periods that correspond to bins of light ($\pm 200 \mu\text{mol m}^{-2} \text{s}^{-1}$) and temperature ($\pm 1 \text{ K}$) at the Castelporziano measurement site.

10

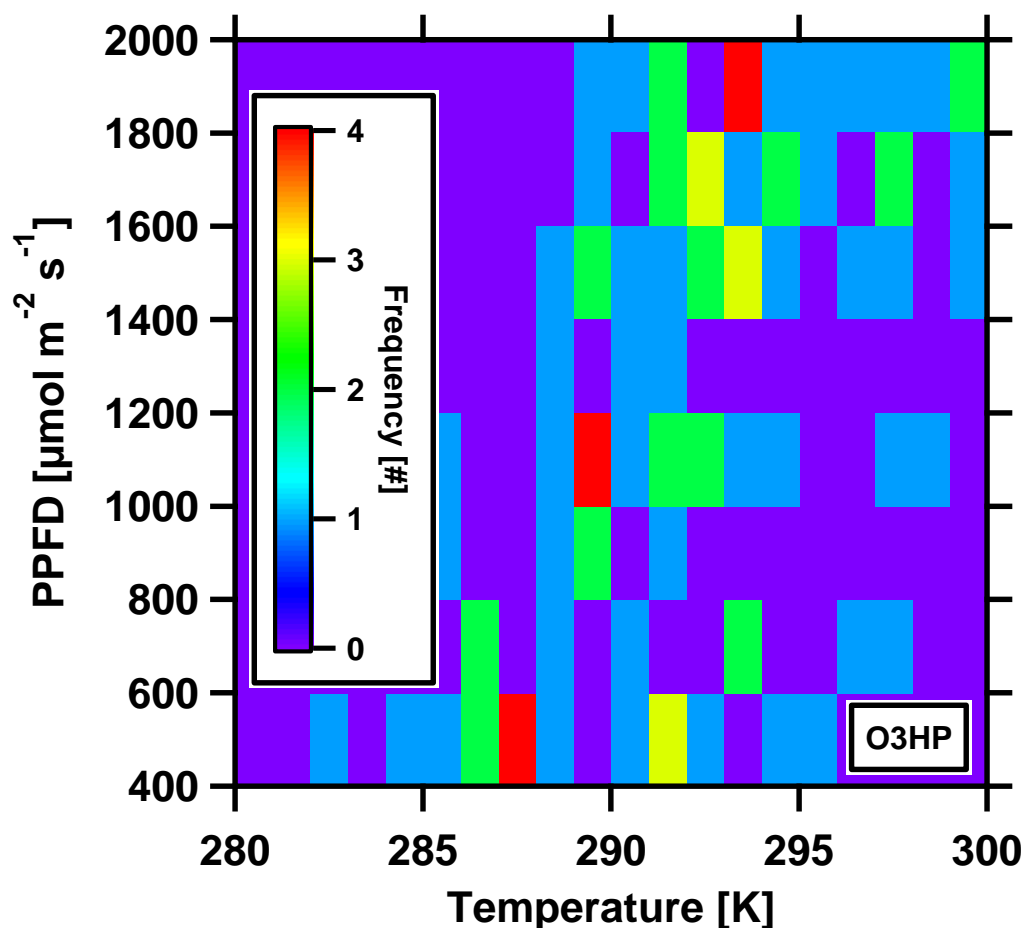


Figure S14 Two dimensional histogram plot of flux averaging periods that correspond to bins of light ($\pm 200 \mu\text{mol m}^{-2} \text{s}^{-1}$) and temperature ($\pm 1 \text{ K}$) at the O3HP measurement site.

5

References

Ferrea, C., Zenone, T., Comolli, R., Seufert, G.: Estimating heterotrophic and autotrophic soil respiration in a semi-natural forest of Lombardy, Italy, *Pedobiologia* 55 (2012) 285– 294.

10

Langford, B., Davison, B., Nemitz, E., and Hewitt, C. N.: Mixing ratios and eddy covariance flux measurements of volatile organic compounds from an urban canopy (Manchester, UK), *Atmos. Chem. Phys.*, 9, 1971-1987, doi:10.5194/acp-9-1971-2009, 2009.

15

Langford, B., Acton, W., Ammann, C., Valach, A., and Nemitz, E.: Eddy-covariance data with low signal-to-noise ratio: time-lag determination, uncertainties and limit of detection, *Atmospheric Measurement Techniques*, 8, 4197-4213, 10.5194/amt-8-4197-2015, 2015.

20

Putaud, J. P., Bergamaschi, P., Bressi M., Cavalli, F., Cescatti, A., Daou, D., Dell'Acqua, A., Douglas, K., Duerr, M., Fumagalli, I., Goded, I., Grassi, F., Gruening, C., Hjorth, J., Jensen, N. R., Lagler, F., Manca, G., Martins Dos Santos, S., Matteucci, M., Passarella, R., Pedroni, V., Pokorska, O., Roux, D., JRC – Ispra Atmosphere – Biosphere – Climate Integrated monitoring Station 2013 Report,, EUR 26995 EN, doi: 10.2788/926761, 73-93.

5 Taipale, R., Ruuskanen, T. M., Rinne, J., Kajos, M. K., Hakola, H., Pohja, T., and Kulmala, M.: Technical Note: Quantitative long-term measurements of VOC concentrations by PTR-MS - measurement, calibration, and volume mixing ratio calculation methods, *Atmospheric Chemistry and Physics*, 8, 6681-6698, 2008.

Zhao, J., and Zhang, R. Y.: Proton transfer reaction rate constants between hydronium ion (H_3O^+) and volatile organic compounds, *Atmospheric Environment*, 38, 2177-2185, 2004.

10